An Accurate Model for Seaworthy Container Vessel Stowage Planning with Ballast Tanks

Dario Pacino[1], Alberto Delgado[1], Rune Møller Jensen[1], and Tom Bebbington[2]

[1] IT-University of Copenhagen, Denmark {dpacino,alde,rmj}@itu.dk
[2] Maersk Line Operations, Global Stowage Planning, Singapore
Tom.Bebbington@maersk.com

Abstract. Seaworthy container vessel stowage plans generated under realistic assumptions are a key factor for stowage decision support systems in the shipping industry. We propose a linear model with ballast tanks for generating master plans, the first phase of a 2-phase stowage optimization approach, that includes the main stability and stress moments calculations. Our approach linearizes the center of gravity calculation and hydrostatic data tables of the vessel in order to formulate stability and stress moments constraints that can handle variable displacement. The accuracy level of these linearizations is evaluated when the displacement of the vessel is allowed to change within a small band.

1 Introduction

The past two decades have seen a continuous increase in containerized shipping. Liner shipping companies meet these demands offering a higher frequency of service and deploying larger vessels. As a consequence, the generation of stowage plans (assignments of containers to vessel slots) has become more complex and hard to handle manually, raising the interest of the industry toward computerized aids. Stowage plans are hard to produce in practice. First, they are made under time pressure by human stowage coordinators just hours before the vessel calls the port. Second, deep-sea vessels are large and often require thousands of container moves in a port. Third, complex interactions between low-level stacking rules and high-level stress limits and stability requirements make it difficult to minimize the makespan of cranes and, at the same time, avoid that containers block each other (overstowage). In a previous work, [7], we have developed a stowage planning optimization approach that, similar to the most successful current approaches (e.g, [9, 5, 1]), decomposes the problem hierarchically as depicted in Figure 1. First the *multi-port master planning* phase decides how many containers of each type to stow in a set of storage areas. Based on this distribution, a complete stowage plan is generated in the *Slot Planning* phase by stowing

Fig. 1: Hierarchical decomposition of stowage planning into master and slot planning.

individual containers. The approach can generate representative stowage plans for up to 10.000 Twenty-foot Equivalent Units (TEU) vessels within 10 minutes (on a 2.0 GHz AMD Opteron), as required for practical usage by the industry.

All of the models present in the literature, however, are based on the assumption that the displacement of the ship (the total weight of the loaded vessel) is constant. Hydrostatic calculations, such as buoyancy, stability, trim and draft restrictions are based on non-linear functions of the ship's center of gravity and vessel displacement. Those can, however, easily be linearized and translated to bounds on the position of the center of gravity when considering a constant displacement. In reality ballast tanks are used by stowage coordinators to better handle the stability of the vessel and allow stowage configurations that are otherwise infeasible. Ignoring ballast water can become a great source of error, as it can constitute up to 25% of the ship's displacement. Including tanks in the mathematical models, however, brings forth a number of non-linear constraints due to the, now variable, vessel displacement. When variable displacement is taken into account, the above mentioned hydrostatic calculations become a function of two variables, center of gravity position and displacement. The previously trivial linearization has now become complex and difficult to handle efficiently. The intuition behind this complexity is simple. When the displacement is constant it is possible to pre-calculate the amount of water the vessel will displace. With variable displacement the amount of displaced water changes and causes the buoyancy forces to change non-linearly due to the curved shape of the vessel hull.

In this paper we introduce a linear model for the master planning phase that considers ballast tanks and deals with variable displacement. This model is concerned only with the seawhortiness of the vessel, but can easily be extended to optimize handling of the vessel at port. According to our industrial partner, it is possible for stowage coordinators to make an educated guess on the amount of ballast water that a vessel might need within 15% from the actual amount. We use this assumption to define a displacement range within which we are able to formulate a linearization of the stability constraints within an acceptable error. We analyse the accuracy of our model experimentally on 10 real instances provided by our industrial partner. Our analysis suggests that within 5% of the current displacement of the vessel, our calculations are accurate enough for the master plans to be seaworthy. The analysis also indicates a direct relation between the size of the variation in the displacement of the vessel and the error on the center of gravity and the linearizations depending on it.

The remainder of the paper is organized as follows. Section 2 describes the problem. Section 3 introduces related work. Section 4 presents our model. Section 5 and 6 present the analysis and conclusions.

2 Background and Problem Statement

ISO containers transported on container ships are normally 8' wide, 8'6" high, and either 20', 40', or 45' long. *High cube* containers are 9'6" high and *pallet*

wide containers are slightly wider and can only be placed side-by-side in certain patterns. Refrigerated containers (*reefers*) must be placed near power plugs. Containers with dangerous goods (*IMO containers*) must be placed according to a complex set of separation rules. The capacity of a container ship is given in TEU. As shown in Figure 2, the cargo space of a vessel is divided into sections called *bays*, and each bay is divided into an *on deck* and a *below deck* part by a number of *hatch-covers*, which are flat, leak-proof structures. Each sub-section of a bay consists of a row of *container stacks* divided into *slots* that can hold a 20' ISO container. Figure 3 (a) and (b) show the container slots of a bay and stack, respectively. Stacks have max height limit and different weight limits. Two weight limits exists for each stack, one regarding the outer container supports and one regarding the inner supports. Limits on the inner supports are often the smallest as the vessel structure in the middle of a stack is weaker. The inner supports are used only when 20 containers are stowed as depicted in Figure 3 (b). When 20 and 40 containers are mixed in the same stack, only half of the 20 weight is considered to be supported by the outer supports, since the other half sits on the inner supports. Below deck, cell guides secure containers transversely. Containers on deck are secured by lashing rods and twist locks with limited strength. Thus, container weights must normally decrease upwards in stacks on deck. Moreover, lashing rods of 20' stacks must be accessible and stack heights must be under the vessel's minimum line of sight. 45' containers can normally only be stowed over the lashing bridge on deck.

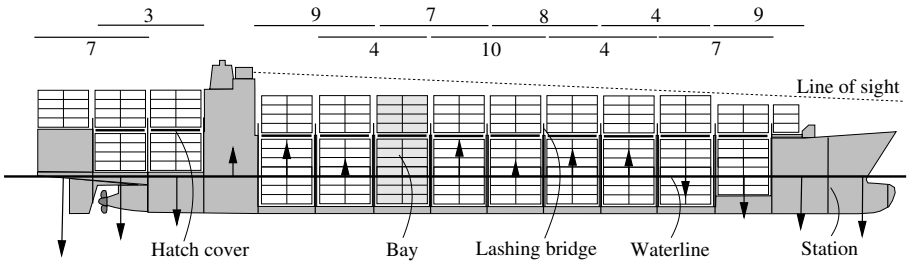

Fig. 2: Arrangement of container vessel bays. The vertical arrows show an example of the resulting forces acting on the ship sections between calculation points (stations). Single crane work hours for adjacent bays are shown at the top.

A container ship must sail at even keel and have sufficient *transverse stability*. Figure 3(c) shows a cross section of a ship. For small inclination angles, the volume of the emerged and immersed water wedges (shaded areas) and thus the distance GZ are approximately proportional with the angle such that the buoyancy force intersects the center line in a fixed position called the *metacenter*, M [8]. For an inclination angle θ, the ship's uprighting force is proportional to $GZ = GM \sin\theta$. GM is called the *metacentric height* and the center of gravity G must be on the center line and result in sufficient GM for the ship to be stable. Maximum and minimum draft restrictions apply due to port depths, working height of cranes, and the propeller. The *trim* is the difference between the aft and fore draft and must be kept within a given span. For a station position p,

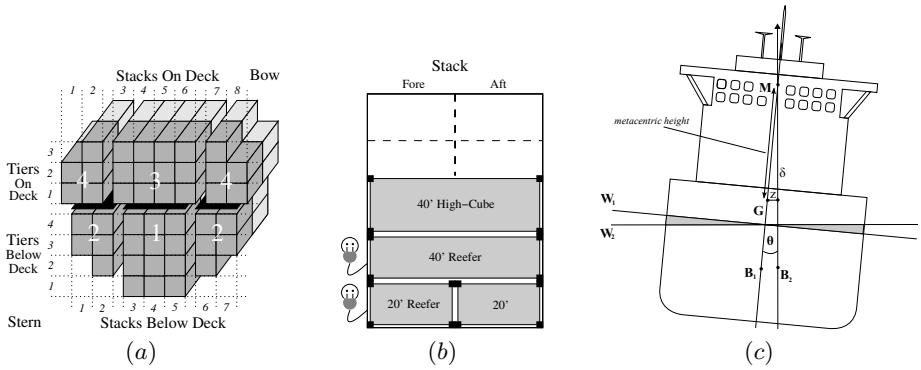

(a) (b) (c)

Fig. 3: (a) A bay seen from behind. (b) A side view of a stack of containers. Power plugs are normally situated at bottom slots. (c) Transverse stability.

the *shear force* is the sum of the resulting vertical forces on vessel sections (see Figure 2) acting aft of p, and the *bending moment* is the sum of these forces times the horizontal distance to them from p. Both of these stresses must be within limits. The vessel also has transverse bending moment (*torsion*) limits. Given the displacement and longitudinal center of gravity (lcg) of a vessel, the metacenter, draft, trim, and the buoyancy of each section of the vessel can be derived from hydrostatic tables. Ballast tanks distributed along the vessel are used to modify displacement and center of gravity by pumping water in or out of the tanks, changing metacenter, draft, trim, and buoyancy of each section.

A container ship transports containers between ports on a fixed cyclic route. A *stowage plan* assigns the containers to load in a terminal to slots on the vessel and it is often sent to the terminal shortly before calling it. It is the liner shippers, and not the port terminals, that are in charge of producing stowage plans. It is impractical to study large optimization models that include all details of stowage planning. On the other hand, all major aspects of the problem must be modeled for the results to be valuable. For container types this includes 20', 40', and reefer containers. In addition, since stability, trim, draft and stress moment limits should not fully be ignored, some weight classes of containers must be introduced. It is also important to take into consideration the containers already onboard the vessel when arriving at the current port.

3 Literature Review

Even though several of the publications on stowage planning available in the past years address stability and stress moments, very few present Linear/Integer programming models that incorporate them as constraints or objectives. Additionally, none of them consider variable displacement due to ballast tanks. The most complete formulation of stability and stress moments as part of a Integer Programming (IP) model is introduced in [4]. Though their model is not solved in practice, due to its complexity, it constrains GM, transversal stability (heel

angle), trim, shear forces, and bending moments. Linearizations depending on the displacement of the vessel, made variable due to the inclusion of the loading and unloading sequence of containers into the model, are suggested for the stability constraints. No evaluation of the impact of these linearizations is presented, probably due to the fact that their model was not used in practice. Shear forces and bending moments are addressed, but they disregard the impact of the cargo in the buoyancy force. The IP formulations introduced in [2, 6] determine in which vessel slot to load each container in the loadlist. These models handle transversal stability and trim by constraining the weight difference between transversal (left and right) and horizontal (bow and stern) sections of the vessel to be within certain tolerance. The GM is constrained by not allowing heavy containers on top of light ones, a rule of thumb used in the industry for some vessels, but that does not necessarily generalize to all kinds of vessels. In [5], a model that distributes types of containers to sections of the vessel is introduced. This model constrains the center of gravity of the vessel with respect to precomputed constants to satisfy GM, trim, and transversal stability constraints. To the best of our knowledge, the only approach available in the literature that considers the use of ballast tanks is presented in [3]. A heuristic uses ballast water to bring the longitudinal center of gravity within a permissible range defined based on the trim desired. Later, a local search is used to fix the GM.

4 Stability and Stress Model with Ballast Tanks

The introduction of ballast tanks into the optimization model causes the displacement of the vessel to become variable. This makes the calculation of the center of gravity non-linear and thus, it is no longer possible to use the linearization of the hydrostatic data from our previous work. Two major non-linearities must be handled once variable displacement has to be modelled. First, the calculation of the center of gravity, and second the linearization of the hydrostatic data. Consider the calculation of lcg without ballast tanks: $\frac{LM^o+\sum_{l\in L} G_l^L v_l}{W}$, where LM^o is the constant longitudinal moment of the vessel, G_l^L is the lcg and v_l is the weight of a location $l \in L$, and W is the displacement given by $W = W^o + \sum_{l\in L} v_l$, where W^o is the constant weight of the vessel. Since all containers in the loadlist are loaded, the displacement is constant, which makes the calculation linear. Now consider the same calculation where we include ballast tanks as a variable: $\frac{LM^o+\sum_{l\in L} G_l^L v_l+\sum_{u\in U} G_u^L v_u}{W+\sum_{u\in U} v_u}$, where U is the set of ballast tanks, G_u^L is their lcg, and v_u is the variable defining the amount of water to be loaded in tank $u \in U$. Since the amount of water in the tanks is not known a priori, the displacement of the vessel is now no longer constant, and the calculation becomes non-linear. In order to deal with this, we propose the following approximation:

$$LCG = \frac{LM^o + \sum_{l\in L} G_l^L v_l + \sum_{u\in U} G_u^L (v_u + \Delta_u)}{W + W^T + \sum_{u\in U} \Delta_u} \tag{1}$$

$$\approx \frac{LM^o + \sum_{l\in L} G_l^L v_l + \sum_{u\in U} G_u^L (v_u + \Delta_u)}{W + W^T}, \tag{2}$$

where we model the stowage coordinator estimation error with the variables Δ_u, thus the total displacement becomes $W + W^T + \sum_{u \in U} \Delta_u$, where W^T represents the amount of water that we expect to remain constant. We then make a linear approximation of the vessel lcg by removing the allowed changes of ballast water from the denominator of the fraction resulting in equation (2). Given the total capacity of the tanks (W^T) and the fact that the constant weight of an empty vessel $W^o \approx 2W^T$ and that the weight of the cargo $W^C \approx 6W^T$, we can reasonably assume that the error in the approximation of the lcg, given that stowage coordinators can estimate the ballast within 15 percent accuracy, is less than $0.15W^T/(2W^T + 6W^T + W^T) = 1.7\%$. Note that the same approximation can be used to calculate the vertical and transversal center of gravity.

The assumption that the amount of ballast water lies within a given interval is useful for the linearization of the hydrostatic calculations. Hydrostatic calculations are in practice linear approximations of given data points. When the center of gravity and the displacement of the vessel are known, the linearization is very accurate. For the problem we are going to model, this is, however, not the case since both the center of gravity and the displacement can vary. Figure 4 shows a plot of the hydrostatic data for the trim and metacenter calculation. The functions are clearly non-linear. Notice that within a small displacement interval it is possible, however, to approximate the functions accurately with a plane. This is only true for displacement levels that are not at the extremes of the data tables, but it is reasonable to assume that the displacement of a stowage plan will be within these extremes. The planes described above can be defined by the limited ballast water change and thus be used in our model. The

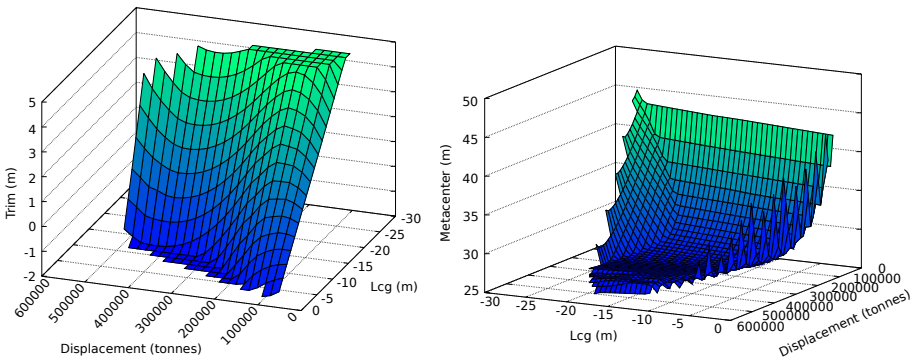

(a) (b)

Fig. 4: (a) Trim as a function of displacement and lcg (b) Metacenter as a function of displacement and lcg.

buoyancy of a vessel is the volume of water that the vessel displace. In order to calculate this volume, it is necessary to know the shape of the vessel hull. For this purpose, the hydrostatic data tables provide the possibility of calculating the submerged area of a vessel at a specific point called a *station*. Figure 5 shows an example of such areas and how stations are distributed along the vessel. Given

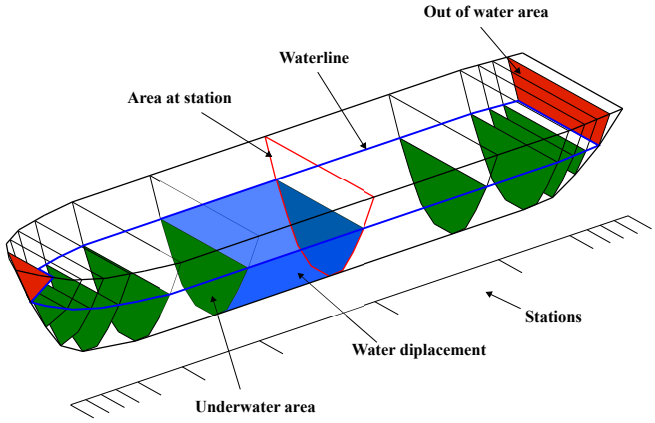

Fig. 5: Areas for buoyancy calculation and stations distribution

two adjacent stations, s_1 and s_2, the buoyancy of the vessel section between the two stations is approximated by $\frac{(A_{s1}+A_{s2})D(s_1,s_2)\delta^W}{2}$, where A_s is the underwater area at station s from now on called *bonjean*, $D(s_1, s_2)$ is the distance between the two stations and δ^W is the density of the water. As Figure 5 shows, stations are not evenly distributed along the vessel. A greater concentration is found at the vessel's extremities, where the hull changes the most. Figure 6 shows two plots of the hydrostatic data related to the bonjean of a station at bow and a station in the middle of a vessel. As expected, the function describing the hull at bow is highly non-linear since the hull greatly changes, which is not the case for stations in the middle of the vessel. Within specific displacement ranges, it is still possible to approximate the function linearly. Should one want to model displacement ranges that include the most non-linear parts, piece-wise linear approximations with a few binary variables can be used.

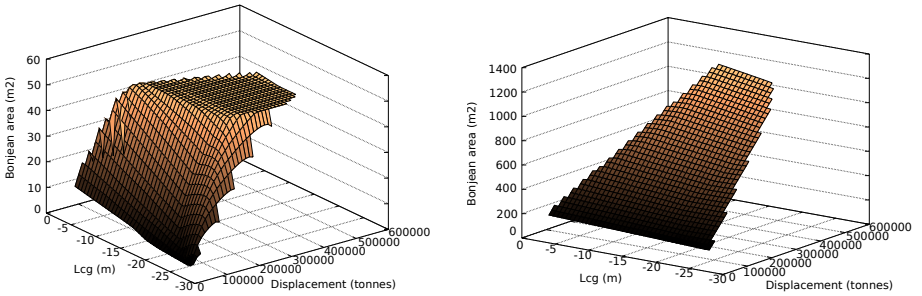

(a) (b)

Fig. 6: (a) Underwater area as a function of displacement and lcg at a bow station (b) Underwater area as a function of displacement and Lcg at a middle station.

4.1 A Linear Model

Following the linear approximation described in the previous section, we propose a refined Linear Programming (LP) model for the master planning phase that includes ballast tank modeling. We constrain ourselves, without loss of generality, to analyse the model for one loading port and several discharge ports. Objectives that focus on efficiency of the master plan (described in [7]) are not included in the model under analysis as they do not have any influence on the seaworthiness of the vessel, and are thus irrelevant to this study.

The multi-port master planning phase assigns types of containers to subsections of bays (*locations*). Figure 3(a) shows four locations within a bay. Outer locations are symmetrically split (such as locations 2 and 4 in the Figure) to ease transverse stability calculations. For 20' and 40' containers, we consider a set of four mutually exclusive container types $T = \{L, H, RL, RH\}$, respectively light and heavy containers and light and heavy reefer containers. Notice that the container types T are only a classification and thus are not bound to fixed weight ranges. For each type $\tau \in T$ the average weight of the containers going to a specific discharge port $p \in P$ is calculated and represented by the constants $W_p^{20\tau}$ and $W_p^{40\tau}$, thus causing a more refined weight categorization than taking the average weight of the containers in each container class. We define two sets of decision variables, $x_{pl}^{20\tau}$ and $x_{pl}^{40\tau}$, representing respectively the amount of 20' and 40' containers of type $\tau \in T$ to be stowed in location $l \in L$ going to port $p \in P$, where L is the set of all locations. Given the set U of ballast tanks in a vessel, we define a set of decision variables, $x_u \in \mathbb{R}$, representing the amount of water present in the tanks. We then propose the following LP model:

minimize

$$\sum_{u \in U} y_u \tag{3}$$

subject to

$$\sum_{p \in P} \sum_{\tau \in T} \left(x_{pl}^{20\tau} + 2x_{pl}^{40\tau} \right) \leq C_l \quad \forall l \in L \tag{4}$$

$$\sum_{p \in P} \sum_{\tau \in T} x_{pl}^{\alpha\tau} \leq C_l^{\alpha} \quad \forall l \in L, \alpha \in \{20, 40\} \tag{5}$$

$$\sum_{p \in P} \sum_{\tau \in \{RL, RH\}} \left(x_{pl}^{20\tau} + x_{pl}^{40\tau} \right) \leq C_l^{RS} \quad \forall l \in L \tag{6}$$

$$\sum_{p \in P} \sum_{\tau \in \{RL, RH\}} \left(0.5x_{pl}^{20\tau} + x_{pl}^{40\tau} \right) \leq C_l^{RC} \quad \forall l \in L \tag{7}$$

$$\sum_{p \in P} \sum_{l \in L} x_{pl}^{\alpha\tau} = LD^{\alpha\tau} p \quad \forall \tau \in T, \alpha \in \{20, 40\} \tag{8}$$

$$\sum_{p \in P} \sum_{\tau \in T} W_p^{\alpha\tau} x_{pl}^{\alpha\tau} = v_l^{W\alpha} \quad \forall l \in L, \alpha \in \{20, 40\} \tag{9}$$

$$v_l^{W20} \leq W_l^{20} \quad \forall l \in L \tag{10}$$

$$0.5v_l^{W20} + v_l^{W40} \leq W_l^{40} \quad \forall l \in L \tag{11}$$

$$v_l^{W20} + v_l^{W40} = v_l^{W} \quad \forall l \in L \tag{12}$$

$$\sum_{u\in U} x_u + \sum_{l\in L} v_l^W + W^o = v^W \tag{13}$$

$$x_u \leq C_u \quad \forall u \in U \tag{14}$$

$$(E_u - \epsilon) \leq x_u \leq (E_u + \epsilon) \quad \forall u \in U \tag{15}$$

$$\frac{\sum_{l\in L} G_l^L v_l^W + \sum_{u\in U} G_u^L x_u + LM^o}{W} = v^{Lcg} \tag{16}$$

$$\frac{\sum_{l\in L} G_l^V v_l^W + \sum_{u\in U} G_u^V x_u + VM^o}{W} = v^{Vcg} \tag{17}$$

$$\mathcal{L}^{Trim-} \leq A_T^W v^W + A_T^{Lcg} v^{Lcg} + A_T \leq \mathcal{L}^{Trim+} \tag{18}$$

$$\mathcal{L}^{DraftA-} \leq A_{DA}^W v^W + A_{DA}^{Lcg} v^{Lcg} + A_{DA} \leq \mathcal{L}^{DraftA+} \tag{19}$$

$$A_{DF}^W v^W + A_{DF}^{Lcg} v^{Lcg} + A_{DF} \leq \mathcal{L}^{DraftF+} \tag{20}$$

$$A_M^W v^W + A_M^{Lcg} v^{Lcg} + A_M = v^M \tag{21}$$

$$v^M - v^{Vcg} \geq \mathcal{L}^{GM-} \tag{22}$$

$$\delta^W D_{(i,j)} \frac{\sum_{s\in\{i,j\}} A_{Bs}^W v_{p0}^W + A_{Bs}^{Lcg} v^{Lcg} + A_{Bs}}{2} = v_{(i,j)}^B \quad \forall (i,j) \in S \tag{23}$$

$$W_f^\alpha + \sum_{l\in L} p_{lf}^\alpha v_l^W + \sum_{u\in U} p_{uf}^\alpha x_u \; - \sum_{s\in S} p_{sf}^\alpha v_s^B = v_f^{S\alpha} \quad \forall f \in F, \alpha \in \{Aft, Fore\} \tag{24}$$

$$M_f^\alpha + \sum_{l\in L} a_{lf}^\alpha p_{lf}^\alpha v_l^W + \sum_{u\in U} a_{uf}^\alpha p_{uf}^\alpha x_u - \sum_{s\in S} a_{sf}^\alpha p_{sf}^\alpha v_s^B = v_f^{B\alpha} \; \forall f \in F, \alpha \in \{Aft, Fore\} \tag{25}$$

$$\mathcal{S}_f^- \leq w_f v_f^{sFore} + (1 - w_f) v_f^{SAft} \leq \mathcal{S}_f^+ \tag{26}$$

$$\mathcal{B}_f^- \leq w_f v_f^{BFore} + (1 - w_f) v_f^{BAft} \leq \mathcal{B}_f^+ \tag{27}$$

$$E_u - x_u \leq y_u \quad \forall u \in U \tag{28}$$

$$x_u - E_u \leq y_u \quad \forall u \in U \tag{29}$$

All the weight limits and capacities of the model have been reduced to account for onboard containers. The TEU capacity of each location, C_l, is enforced by constraint (4). Location specific capacity requirements regarding the length of the containers (C_l^{20} and C_l^{40}) are enforced using constraint (5). Constraint (6) and (7) limit, respectively the total number of reefer TEU (C_l^{RS}) and Forty-foot Equivalent Units (FEU) (C_l^{RC}) used. Constraint (8) ensures that all containers are loaded.With constraint (9), we define the variables v_l^{W20} and v_l^{W40}, holding respectively the weight of the 20'and 40' containers in location $l \in L$. Weight limitations for the 20' (W_l^{20}) and 40' W_l^{40} containers are guaranteed by constraints (10) and (11). Constraint (12) defines the auxiliary variable v_l^W representing the weight of location $l \in L$. The displacement of the vessel is represented by the auxiliary variable v^W with constraint (13) where W^o is the constant weight of the vessel. Note that the constant weight of the vessel also includes the weight of the onboard containers. Constraint (14) defines the capacity (C_u) of the tanks, while given E_u as the initial condition of the tanks constraint (15) defines the allowed ϵ ballast change. Variable v^{Lcg} represents the lcg of the vessel and is computed in constraint (16) using the approximation defined in (2). The constant LM^o is the constant longitudinal moment of the vessel, including onboard containers, G_l^L is the lcg of location $l \in L$, G_u^L is the

lcg of tank $u \in U$, and W is the approximated constant displacement. The same approximation is used in constraint (17) for the calculation of the vertical center of gravity (vcg) represented by the variable v^{Vcg}. Constraint (18) represents the linearized hydrostatic calculation of trim. Given the displacement of the vessel v^W and its lcg v^{Lcg}, constraint (18) approximates the plane with the coefficients A_T^W, A_T^{Lcg} and A_T. The calculated trim is then kept within the limits $\mathcal{L}^{Trim-}$ and $\mathcal{L}^{Trim+}$. Changing the coefficients accordingly, constraint (19) and (20) approximate the draft aft and fore of the vessel. Both drafts are kept within the maximum limits $\mathcal{L}^{DraftA+}$ and $\mathcal{L}^{DraftF+}$. Due to the propeller it is also necessary to constrain the draft aft to be at a minimum depth $\mathcal{L}^{DraftA-}$. The metacenter is also calculated using the hydrostatic approximation and it is defined in constraint (21) by the variable v^M. The GM is then calculated in constraint (22) and kept above the security limit $\mathcal{L}^{GM}$. The buoyancy of the section of a vessel between two adjacent stations is defined in constraint (23) by the variable $v^B_{(i,j)}$. The set S is the set of adjacent station pairs (i, j), $D_{(i,j)}$ is the distance between the two stations, and δ^W is the density of the water. In the shear and bending calculations, we take into account the forces aft or fore of a frame. Since frames do not always coincide with the starting points of tanks, locations or buoyancy stations, it is necessary to know given a frame (a fixed calculation point) $f \in F$ the faction of weight that needs to be taken into account from a location l, tank u or station s. For this purpose the constant $p_{lf}^{Aft} \in [0, 1]$ is used to denote the fraction of cargo to be considered from location $l \in L$ aft of frame $f \in F$ and p_{lf}^{Fore} for the fraction fore of the frame ($p_{uf}^{Aft}, p_{uf}^{Fore}$ for the tanks and $p_{sf}^{Aft}, p_{sf}^{Fore}$ for the buoyancy). Since the shear forces and bending moments are calculated per frame, errors from the linearization are accumulated the further away from the calculation frame that the weights are. This can become very problematic in the case of bending, where the forces are multiplied by the arm, increasing the approximation error substantially. Shear and bending calculations can be done for either fore or aft part of a frame. A more precise modelling of stress forces requires the calculation at both the aft and fore part of a frame, where the two resulting stresses are blended such that aft calculations are weighted more at the stern and less at the bow. Constraint (24) calculates the shear forces both aft and fore of each frame $f \in F$ and defines the shear variable v_f^S, and where W_f^α is the constant weight aft or fore of frame f. The final shear calculation, where the aft and fore shear are mixed using a scaling factor $w_f \in [0, 1]$ (such that it is 1 for the first frame at bow and 0 in the first frame at stern) is kept within the limits $\mathcal{S}_f^+$ and $\mathcal{S}_f^-$ in constraint (26). The same calculation is made for the bending. The bending variable $v_f^{B\alpha}$ is defined in constraint (25), where $a_{lf}^\alpha, a_{uf}^\alpha, a_{sf}^\alpha$ are respectively the arm to frame $f \in F$ of location $l \in L$, tank $u \in U$ and buoyancy section $s \in S$ for both the aft and fore calculation. The constant moment of the vessel is given by the constant M_f^o and bending is kept within the limits $\mathcal{B}_f^+$ and $\mathcal{B}_f^-$ by constraint (27). Constraints (28) and (29) define the cost variable y_u quantifying the changes in tank configuration from the initial estimate. The accuracy of the approximations decreases with the extend of the change in ballast water. Thus, objective (3) minimizes this change.

Instances Characteristics								
ID	TEU (%)			Weight (%)			Displacement (10^3 tons)	Tanks (10^3 tons)
	Total	Release	Load	Total	Release	Load		
1	92	39	53	32	13	19	149	5
2	74	37	37	45	23	23	176	8
3	60	18	41	42	12	30	169	7
4	81	29	52	53	20	33	192	7
5	66	13	52	26	8	18	135	11
6	49	18	31	25	9	16	133	11
7	69	28	41	41	17	23	161	5
8	46	13	33	29	8	21	144	10
9	59	25	34	30	14	16	141	5
10	59	20	39	32	10	22	146	7

Table 1: *Characteristics of the test instances.* Starting from the left the columns indicate: the ID of the instance, the total utility percentages in terms of TEU capacity used, thereof the percentage of containers in the release and in the loadlist. The next three columns indicate percentages of utilization in terms of weight, in total, for the containers in the release and in the loadlist. The initial displacement and the estimated ballast water are given by the last two columns.

5 Analysis of Model Accuracy

The model has been evaluated experimentally on a case study of 10 industrial stowage plans for a vessel of approximately 15.000 TEUs. The linear approximations used by the LP model for the generated solutions are compared with exact manual calculations. Table 1 gives an overview of the instances' characteristics.

We performed experiments allowing different changes in displacement and observed how the accuracy of the model changes accordingly. First we consider the linear approximation about the center of gravity of the vessel.

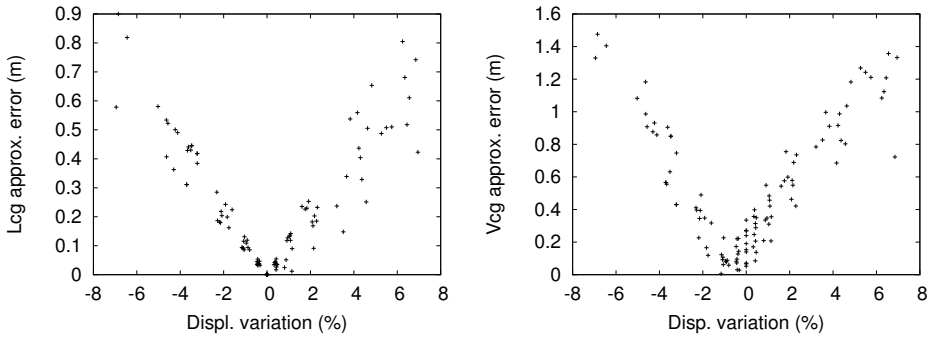

(a) (b)

Fig. 7: (a) Error in the lcg. (b) Error in the vcg.

Figure 7 shows two graphs describing how the approximation of the longitudinal (a) and vertical (b) center of gravity behaves as the displacement changes. For both graphs, the horizontal axis represents the change of displacement in percentage, while the vertical axis represents the error in meters. Each point in the graph is generated by forcing changes in the ballast water of the 10 test instances. In Figure 7a it is possible to see, as expected, that when the displace-

ment is unchanged, the value of the lcg is accurate and the more the displacement moves away from its true value the less accurate the approximation becomes. Note that for a displacement range of 5 percent, the calculation inaccuracy is at most 0.3 meters and is thus, still very accurate for practical usage. The calculations for the vcg are not as accurate (Figure 7b). Within the 5 percent range, the linearized value is, however, at most 0.8 meters from the correct one. This was an expected result, as it is not possible to precisely estimate the vcg of, for example, locations since we do not know where the containers will be stowed. The accuracy error of the vcg is, however, still very small.

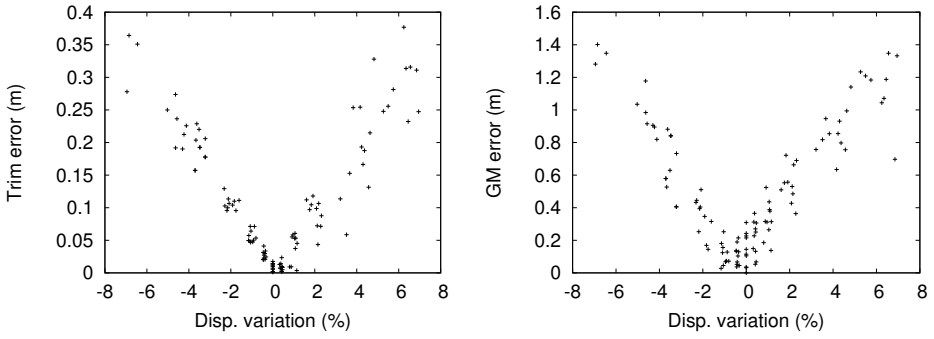

(a) (b)

Fig. 8: (a) Error for the trim (b) Error for the GM.

Now that we have shown that linearizations for the center of gravity are accurate, we focus on analyzing the accuracy of the hydrostatic data linearization. In Figure 8 we use the same graph as before with the horizontal axis describing the percentage displacement changes and the vertical axis the calculation error. Figure 8a represents the error for the trim which, as it can be seen, is very small. Within a 5 percent displacement range, the error is at most 15 centimeters. Figure 8b shows the same analysis for the calculation of GM. Notice that both for the trim and GM calculations, an error is present even at constant displacement. The error we see is due to the linearization of the hydrostatic functions. For GM it also includes the approximation error of the vcg.

We now move our focus to the linearization of the bonjean areas which we expect to be the most inaccurate. Figure 9a shows the same analysis we have done so far for the bonjean areas. The graph shows the maximum error over all bonjean areas as a function of the displacement changes. As can be seen, the variation in displacement is not the main source of error. Most of the inaccuracy is due to the linearization of the hydrostatic data. Figure 9b shows how the bonjean error is concentrated at the extremities of the vessel where the hull changes most. The horizontal axis represents the position of the station on the vessel (where 0 is at bow) and the vertical axis is the bonjean error. Notice that the largest errors are found for stations at the bow. This can be explained by the fact that the range of drafts in our test data forces the linearization of these

bonjean areas to be right by the inflection point of the hydrostatic curve (see figure 6a) where the linearization is most inaccurate. Better approximations can then be expected for larger drafts, as it is the case for the bonjean of the stations at the stern. The inaccuracy of the bonjean is, however, still quite small if we consider that the in the worst case, there is an error of only 4 square meters over an area of over 111 square meters.

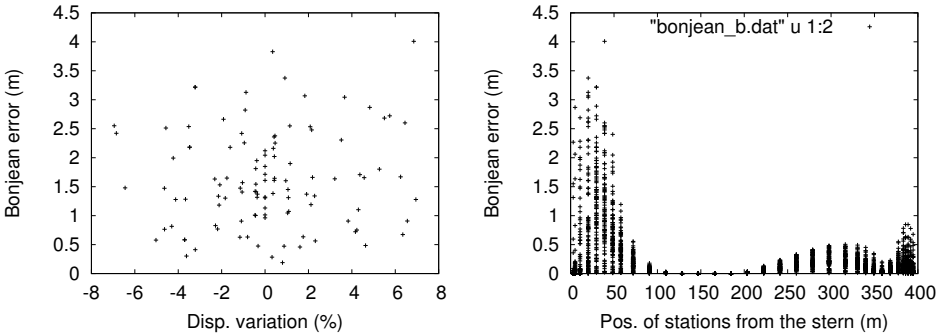

(a) (b)

Fig. 9: (a) Approximation error of the total bonjean as a function of displacement change (b) Approximation error of the bonjean areas per station.

Shear forces and bending moment calculations depend on the buoyancy of the vessel which in turn is calculated using the bonjean approximations. Figure 10a shows, in the same way as the other graphs, how the percentage error in the shear calculation (the vertical axis) behaves as a function of the variation of the displacement (the horizontal axis). As expected, the dominant error is not the approximation of the center of gravity of the vessel since the inaccuracy is more or less the same independently of how much the displacement changes. A more tight relation can be seen when the shear calculation is related to the error in the bonjean linearization. Figure 10b shows the percentage error of the shear force calculation as a function of the total error in bonjean area from the hydrostatic linearization. As depicted, the error in the shear calculation increases with the error in the bonjean linearization. The graph also groups the data points according to their displacement range, and for the data points with no displacement change we can see that the tendency remains the same. One must also take into account that the linearization error of the bonjean is amplified in the shear foces calculation by the fact that it becomes accumulated in the summation of the forces. This particular information is very important when analyzing the error in the bending moment calculation, since this accumulated error is multiplied by the arm of the moment and thus multiplies its impact.

Figure 11a shows the error in the bending calculation as a function of the changes in displacement. As expected, like for the shear force calculation, the main source of error is not the approximation of the lcg, but rather the error in the linearization of the bonjean areas. Due to the fact that the bonjean error

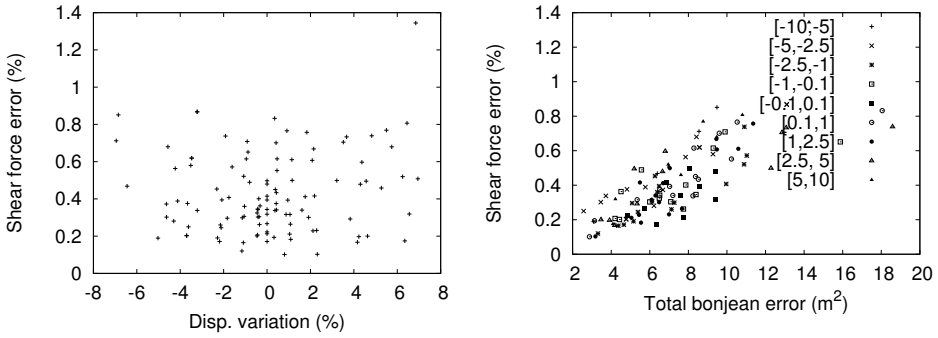

(a) (b)

Fig. 10: Approximation error of the shear forces as (a) a function of displacement change, and (b) a function of the total bonjean error.

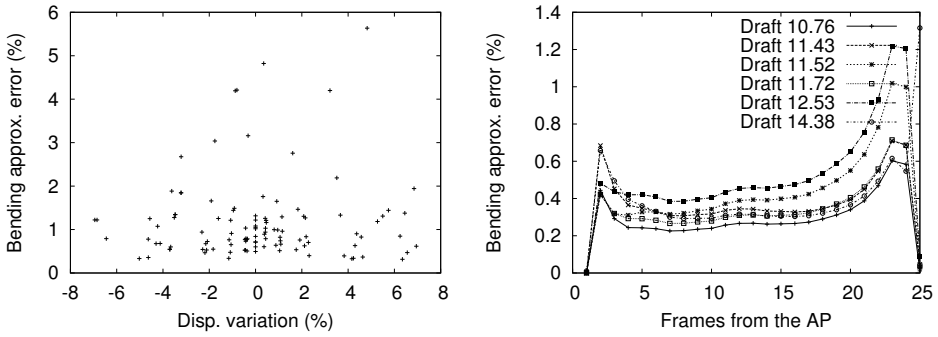

(a) (b)

Fig. 11: Approximation error of the bending moment (a) as a function of displacement change, and (b) at each bonjean station for constant displacement.

is amplified by the multiplication of the arm, it is necessary to look at the error at each calculation frame in order to see how the error of the bending moment changes. We do this by forcing the displacement to remain constant, thus removing the error of the lcg approximation, and analyzing how the bending error changes at each calculation frame as the draft of each of the 10 test instances changes. The result is shown in Figure 11b, where the horizontal axis represents the frames of the vessel and the vertical axis is the percentage of error in the bending moment calculation. Each of the lines plotted in the graph represent one of the 10 test instances each of which has a different draft. As expected the bending moment is less accurate at the bow and stern due to the imprecision in the bonjean calculations. One more thing worthy of notice is that there is no direct relation between the bending error and the draft of the vessel. This is due to the non-linear shape of the hull. The bending error for constant displacement does not exceed 1.4 percent, however, when variable displacement is considered an error of up to 3.5 percent might be reached within a 5 percent displacement

variation. We consider these approximations acceptable. Higher accuracy can be achieved by reducing the linearization error of the hydrostatic functions for bonjean.

6 Conclusion

This paper introduced an LP model including ballast tanks for the master planning phase of a 2-phase stowage planning optimization approach. Analysis of 10 real instances show that our model is successful at coping with variable displacement, a feature introduced by the ballast tanks, within an acceptable error tolerance. Within a 5% band of the current displacement, the master plans generated were seaworthy, with the error in stability calculations increasing proportionally to the variability of the displacement. In future work, we plan to introduce piecewise linearizations on the bonjean hydrostatic data to reduce the error in the stress calculations in our model. This must be done carefully since it might be necessary to include Boolean variables that will negatively impact the performance of the solver. A study of the trade-off between the inclusion of piece-wise linearizations and the error reduction must be carried out.

Acknowledgments We would like to thank Wai Ling Hoi, Andreas Hollmann, Kasper Andreasen, and Mikkel Mühldorff Sigurd at Maersk Line for their support of this work. This research is sponsored in part by the Danish Maritime Fund under the BAYSTOW project.

References

1. Ambrosino, D., Anghinolfi, D., Paolucci, M., Sciomachen, A.: An experimental comparison of different heuristics for the master bay plan problem. In: Proceedings of the 9th Int. Symposium on Experimental Algorithms. pp. 314–325 (2010)
2. Ambrosino, D., Sciomachen, A., Tanfani, E.: Stowing a conteinership: the master bay plan problem. Transportation Research Part A: Policy and Practice 38(2), 81–99 (2004)
3. Aslidis, A.H.: Optimal Container Loading. Master's thesis, Massachusetts Institute of Technology (1984)
4. Botter, R., Brinati, M.A.: Stowage container planning: A model for getting an optimal solution. In: Proceedings of the 7th Int. Conf. on Computer Applications in the Automation of Shipyard Operation and Ship Design. pp. 217–229 (1992)
5. Kang, J., Kim, Y.: Stowage planning in maritime container transportation. Journal of the Operations Research Society 53(4), 415–426 (2002)
6. Li, F., Tian, C., Cao, R., Ding, W.: An integer programming for container stowage problem. In: Proceedings of the Int. Conference on Computational Science, Part I. pp. 853–862. Springer (2008), LNCS 5101
7. Pacino, D., Delgado, A., Jensen, R.M., Bebbington, T.: Fast generation of near-optimal plans for eco-efficient stowage of large container vessels. In: Proceedings of the Second International Conference on Computational Logistics (ICCL'11). pp. 286–301. Springer (2011)

8. Tupper, E.C.: Introdution to Naval Architecture. Elsevier (2009)
9. Wilson, I.D., Roach, P.: Principles of combinatorial optimization applied to container-ship stowage planning. Journal of Heuristics (5), 403–418 (1999)